Neurología xxx (xxxx) xxx—xxx

NEUROLOGÍA

www.elsevier.es/neurologia

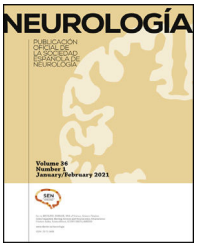

Kernohan-Woltman notch phenomenon: an exceptional neurological picture?

R. Carrasco Moro[a,*], J.M. Pascual Garvi[b], C. Vior Fernández[a], E.E. Espinosa Rodríguez[c], G. Martín Palomeque[d], L. Cabañes Martínez[d], M. López Gutiérrez[e], A. Acitores Cancela[a], E. Barrero Ruiz[a], J.S. Martínez San Millán[f]

[a] *Servicio de Neurocirugía, Hospital Universitario Ramón y Cajal, Madrid, Spain*
[b] *Servicio de Neurocirugía, Hospital Universitario La Princesa, Madrid, Spain*
[c] *Servicio de Neurocirugía, Instituto de Medicina y Cirugía Barcelona, Barcelona, Spain*
[d] *Servicio de Neurofisiología Clínica, Hospital Universitario Ramón y Cajal, Madrid, Spain*
[e] *Servicio de Neurocirugía, Hospital Central de la Defensa Gómez Ulla, Madrid, Spain*
[f] *Servicio de Diagnóstico por Imagen, Hospital Universitario Ramón y Cajal, Madrid, Spain*

Received 15 June 2022; accepted 15 September 2022

KEYWORDS
False localising signs;
Kernohan-Woltman notch phenomenon;
Ipsilateral hemiparesis;
Paradoxical hemiparesis;
Kernohan's notch;
Brain herniation

Abstract
Introduction: Ipsilateral hemiparesis (IH) can be defined as a paradoxical dysfunction of the first motor neuron involving the extremities on the opposite side to that expected, given the location of the triggering intracranial pathology. Compression of the corticospinal tract (CSt) along its course through the contralateral cerebral peduncle against the free edge of the tentorium, known as the Kernohan-Woltman notch phenomenon (KWNP), represents the main cause of IH.
Methods: This retrospective study analyses a series of 12 patients diagnosed with IH secondary to KWNP treated at our institution, including a descriptive study of epidemiological, clinical, radiological, neurophysiological, and prognostic variables.
Results: In 75% of the cases, symptoms had an acute or subacute onset. Initial imaging studies showed signs of significant mass effect in half of the patients, whereas magnetic resonance imaging (MRI) identified a structural lesion in the contralateral cerebral peduncle in two thirds of them. Impairment of the motor evoked potentials (MEP) was verified in 4 patients. During follow-up 7 patients experienced improvement in motor activity, and near half of the cases were classified in the first three categories of the modified Rankin scale.

* Corresponding author.
E-mail address: rodrigo.carrasco@salud.madrid.org (R. Carrasco Moro).

https://doi.org/10.1016/j.nrleng.2022.09.010

Please cite this article as: R. Carrasco Moro, J.M. Pascual Garvi, C. Vior Fernández et al., Kernohan-Woltman notch phenomenon: an exceptional neurological picture? *Neurología*, https://doi.org/10.1016/j.nrleng.2022.09.010

Conclusions: In contrast to prior historical series, most of our patients developed a KWNP secondary to a traumatic mechanism. MRI represents the optimal method to identify both the classic cerebral peduncle notch and the underlying structural lesion of the CSt. The use of MEP can help to establish the diagnosis, especially in those cases lacking definite radiological findings.

PALABRAS CLAVE
Falsos signos localizadores;
Fenómeno de le hendidura de Kernohan-Woltman;
Hemiparesia ipsilateral;
Hemiparesia paradójica;
Hendidura de Kernohan;
Hernia cerebral

Fenómeno de Kernohan-Woltman: ¿un cuadro neurológico excepcional?

Resumen
Introducción: Podemos definir la hemiparesia ipsilateral (HI) como una disfunción de la primera motoneurona que afecta a las extremidades del lado opuesto al esperado, dada la localización de la patología intracraneal desencadenante. La compresión del tracto córtico-espinal (tCE) contra el borde libre del tentorio a su paso por el pedúnculo cerebral se conoce como fenómeno de Kernohan-Woltman (FKW).
Métodos: Estudio retrospectivo de pacientes diagnosticados de HI secundaria a un FKW atendidos en nuestra institución, incluyendo un estudio descriptivo de las variables epidemiológicas, clínicas, radiológicas, neurofisiológicas y pronósticas.
Resultados: En un 75% de los casos la clínica fue de instauración aguda o subaguda. El estudio de imagen inicial mostró signos de efecto de masa significativo en la mitad de los pacientes, mientras que la resonancia magnética (RM) permitió identificar una lesión estructural en el pedúnculo cerebral contralateral en dos terceras partes de los casos. En 4 pacientes se verificó una afectación de los potenciales evocados motores (PEM). Durante el seguimiento, 7 pacientes experimentaron una mejoría de la actividad motora, y aproximadamente la mitad de los casos fueron clasificados en los tres primeros grados de la escala de Rankin.
Conclusiones: En contraste con las series históricas, la mayor parte de nuestros pacientes desarrollaron un FWK a consecuencia de un traumatismo cráneo-encefálico. La RM es la prueba de imagen de elección tanto para identificar la clásica escotadura del pedúnculo cerebral como detectar la presencia de una lesión estructural subyacente. El estudio de PEM puede servir de apoyo al diagnóstico, especialmente en casos dudosos.

Introduction

False localising signs are clinical signs of neurological damage that lead to an erroneous conclusion about the anatomical location of the lesion triggering them.[1] Among them, ipsilateral hemiparesis (IH) has sparked particular interest over the years due to its association with wrong-site craniotomy, especially in the early days of neurosurgery.[2]

Although the Kernohan-Woltman notch phenomenon (KWNP), defined as compression of the contralateral cerebral peduncle against the tentorial notch,[3] is one of the most widely known pathophysiological mechanisms causing IH, its pathogenesis is yet to be fully understood, as most of the available evidence is from isolated case reports or case reviews, with considerable heterogeneity of the reported results.[4,5]

This study provides a detailed description of clinical, radiological, and neurophysiological findings in an original series of patients with IH secondary to KWNP. Our findings are compared against those of the most relevant studies on KWNP.

Material and methods

We retrospectively gathered cases of IH diagnosed between 2000 and 2021. The following data were recorded: *1)* epidemiological data: sex, age (years), manual dexterity, and trigger factor of IH; *2)* clinical data: level of consciousness (Glasgow Coma Scale[6] [GCS]), motor activity of the limbs (modified Medical Research Council [mMRC] scale,[7] except in patients with impaired consciousness, in whom motor response was evaluated with the GCS), and signs of pupillary dysfunction; *3)* brain CT and/or MRI findings: time of study performance, intracranial lesion triggering IH, signs of mass effect, signs of compression of the cerebral peduncles or presence of midbrain lesions (morphological and topographic characteristics, MRI signal alterations), dimensions of the tentorial notch in coronal T2-weighted sections and classification according to the criteria proposed by Adler and Milhorat[8] (narrow [24.5-27 mm], typical [27.1-31.9 mm], or wide [32-39]), and characterisation of other intracranial lesions secondary to trauma or brain herniation; *4)* neurophysiological study results; and *5)* prognosis in terms of motor function and overall clinical status (modified Rankin Scale[9] [mRS]).

Results

Our series included a total of 12 patients. Table 1 presents our sample's epidemiological, clinical, therapeutic, and prognostic characteristics and neurophysiological study results. Table 2 summarises the most relevant imaging findings. All patients were right-handed. No differences were observed in the sex distribution.

Table 1 Clinical characteristics and neurophysiological study results from our series of patients.

Patient	Age/sex	Onset/cause	Neurological examination	Treatment	Progression		mRS	MEP
					Post-surgery	Follow-up		
1	32/♀	SA/right frontal abscess (toxoplasmosis)	GCS 12 (E3V3M6), deterioration to GCS 3	Emergency craniectomy	GCS 15, right hemiparesis (4+/5)	6 m: no motor impairment; 1 y: death (AIDS)	0 (6)	Not performed
2	40/♂	A/aSDH + SAH + depressed skull fracture and right temporal contusion (traffic accident)	GCS 3, bilateral mydriasis, right otorrhagia, epistaxis	Emergency craniotomy	GCS 9[T] (E2V1[T]M6), right hemiparesis (3/5), pyramidal signs + signs of third cranial nerve involvement	2 m: cognitive impairment; right pyramidal signs without motor deficits	2	Not performed
3	23/♂	A/aSDH + right hemisphere contusion (assault)	GCS 3, right mydriasis	Emergency craniectomy	GCS 9[T] (E4V1[T]M4), quadriparesis (right: decer.; left: decort.)	1 y: vegetative state; no motor changes; death (pneumonia)	5 (6)	Not performed
4	62/♂	C/right supra-infratentorial epidermoid cyst	GCS 15, quadriparesis (right: 3/5; left: 4+/5), paresis of lower cranial nerves	Elective craniotomy	No changes	Death (pneumonia)	4 (6)	Impaired central motor conduction, left CST
5	61/♂	SA/postoperative bleeding (right frontal GB, acenocoumarol)	GCS 15, right hemiparesis (4—/5), left residual hemiparesis (4+/5) after surgery for GB	Conservative treatment (steroids)	—	6 m: pyramidal signs without motor deficits; death (GB)	1 (6)	Not performed
6	71/♀	A/right cSDH with rebleeding (fall; acenocoumarol)	GCS 8 (E1V2M5), right hemiparesis (0/5) + right mydriasis	Not treated (cognitive impairment)	—	13 d: death	6	Not performed
7	85/♀	A/left aSDH (spontaneous; acenocoumarol)	GCS 4 (E1V1M4), left decer., left mydriasis	Not treated (cognitive impairment)	—	10 d: death	6	Not performed

Table 1 (*Continued*)

Patient	Age/sex	Onset/cause	Neurological examination	Treatment	Progression		mRS	MEP
					Post-surgery	Follow-up		
8	25/♂	A/diffuse oedema (traffic accident)	GCS 7 (E1V1M5), right decer.	Conservative treatment (neurointensive)	—	6 m: cognitive impairment, right hemiparesis with pyramidal signs (4+/5); 6 y: no improvement	3	Not performed
9	55/♀	A/diffuse oedema + SAH (traffic accident)	GCS 7 (E1V1M5), right hemiparesis (0/5), right mydriasis	Conservative treatment (neurointensive)	—	5 m: cognitive impairment, right hemiparesis with pyramidal signs (0/5) (see Video in Supplementary material)	4	Impaired central motor conduction, left CST
10	16/♂	A/left occipital parenchymal haemorrhage (AVM)	Headache + left hemiparesis (4—/5), deterioration to GCS 6 (E1V1M4), left decer., left mydriasis	Decompressive craniectomy	GCS 15 (E4V4M6), left hemiparesis (4—/5)	10 m: pyramidal signs + tremor + right superior quadrantanopia	1	Not performed
11	58/♀	C/meningioma in greater wing of the left sphenoid bone	GCS 15, motor dysphasia, left hemiparesis (4+/5 brachial, 4—/5 crural)	Elective craniotomy	GCS 15, dysnomia, left hemiparesis (4+/5)	1 y: dysnomia, left pyramidal signs	1	Impaired central motor conduction, right CST
12	47/♀	C/left petroclival meningioma	GCS 15, left hemiparesis (4+/5)	Elective craniotomy (×2)	1) GCS 15, left hemiparesis (0/5) 2) GCS 15, quadriparesis (left: 4—/5, right: 2/5) + involvement of cranial nerves VII—XI	1) 1 w: left hemiparesis (4—/5) 2) 3 m: quadriparesis (left: 4+/5, right: 4—/5)	3	1) Transient loss of right CST signal 2) Loss of left CST signal

A: acute; aSDH: acute subdural haematoma; AVM: arteriovenous malformation; C: chronic; cSDH: chronic subdural haematoma; CST: corticospinal tract; d: day; decer.: decerebrate rigidity; decort.: decorticate rigidity; E: eye response (GCS); GB: glioblastoma; GCS: Glasgow Coma Scale; m: month; M: motor response (GCS); MEP: motor evoked potentials; mRS: modified Rankin Scale; SA: subacute; SAH: subarachnoid haemorrhage; T: tracheostomy; V: verbal response (GCS); w: week; y: year.

Table 2 Neuroimaging findings in our series.

Patient	CT			MRI									
	Time of performance	Mass effect	Peduncle	Time of performance	Peduncular lesion: morphology/topography	T1	T2	FLAIR	GRE	DWI/ADC	DTI	Tentorial notch	Other lesions
1	PreOp	MLS + uncal herniation	Compressed	PostOp (8 days)	Elongated/extensive, ventral-dorsal, lateral + central	↓ ↑ foci	↑	↑	No HS deposition	↑/no DR	Not performed	Not measured	No
2	PreOp	MLS + uncal herniation	Compressed	PostOp (20 days)	Elongated/ventral lateral	Not visible	↑	↑	No HS deposition	Not performed	Not performed	Not measured	DAI
3	PreOp	MLS + uncal herniation	Compressed	PostOp (2 months)	Round/ventral central	↓	↑	↑	Peripheral HS deposition	↓/no DR (↑/peripheral DR)	Not performed	29.8 mm	Ischaemia in right PCA and both ACAs
	PostOp	No	Lesion ↓ density										
4	PreOp	Brainstem displacement	Compressed	PreOp	Peduncle deformation (groove)	–	–	–	No HS deposition	Normal	Not performed	Not measured	No
5	At onset	MLS	Compressed	5 days after onset	Oval/ventral lateral	↓	↑	↑	No HS deposition	Not performed	Not performed	29.5 mm	No
6	At onset	MLS + uncal herniation	Compressed, ↑ density in lateral edge	8 days after onset	Oval/ventral lateral	↓	↑	↑	Not performed	↑/DR	Partial lesion to CST	24.8 mm	No
7	At onset	MLS + uncal herniation	Compressed	Not performed									
8	At onset	MLS + perimesencephalic cistern effacement, petechial haemorrhages	No deformities or lesions	6 months after onset	Oval/ventral lateral	↓	↑	↑	Oval HS deposition	Not performed	Not performed	29 mm	DAI
9	At onset	MLS + perimesencephalic cistern effacement, foci of SAH	No deformities or lesions	2 months after onset	Oval/ventral lateral	Not visible	↑	↑	No HS deposition	↑/DR	Not performed	24.1 mm	DAI, SS
10	PreOp	MLS + uncal herniation	Compressed	PostOp (4 months)	Oval/ventral lateral	Not visible	↑	↑	No HS deposition	↑/DR	Normal CST	28.6 mm	Malacia at surgical site
	PostOp	No	No lesion										
11	PreOp	MLS	Compressed	PreOp	Peduncle deformation (groove)	–	–	–	–	Normal	Not performed	28.1 mm	No
	PostOp	No MLS	No lesion	PostOp (3 months)	Normal	–	–	–	–	Normal	Normal CST	28.1 mm	Malacia at surgical site
12	PreOp	Brainstem displacement	Compressed	PreOp	Peduncle deformation (groove)	–	–	–	–	Normal	Not performed	Not measured	No
	PostOp	No	Lesion ↓ density	PostOp (7 days)	Oval/ventral lateral	↓	↑	↑	No HS deposition	↑/DR	Not performed	28.1 mm	Left pontine ischaemia

ACA: anterior cerebral artery; CST: corticospinal tract; CT: computed tomography; DAI: diffuse axonal injury; DR: diffusion restriction; HS: haemosiderin; MLS: midline shift; MRI: magnetic resonance imaging; PCA: posterior cerebral artery; PostOp: postoperative; PreOp: preoperative; SAH: subarachnoid haemorrhage; ↓: hypointensity; ↑: hyperintensity.

Age ranged from 16 to 85 years (mean: 47.9; median: 50). The initial symptoms were acute or subacute in 75% of patients, caused by head trauma (in 5 patients), intracranial haemorrhage (3), or a rapidly progressive expansive process (an abscess in patient 1). Two-thirds of patients presented impaired consciousness, and half of the sample displayed pupillary dilation. In 10 patients, the initial examination revealed bilateral motor deficits, with more severe involvement in the limbs ipsilateral to the intracranial lesion triggering the symptoms.

All patients underwent CT studies, and all but one underwent MRI (Table 2, Fig. 1). In all cases, the baseline imaging study revealed an intracranial mass effect, which most frequently caused midline shift with or without signs of uncal herniation (50%); other relevant findings included perimesencephalic cistern obliteration secondary to diffuse parenchymatous oedema (patients 8 and 9) and lateral brainstem displacement caused by masses located at the level of the tentorial notch (patients 4 and 12) (Table 2). Imaging studies revealed a structural lesion at the level of the cerebellar peduncle in two-thirds of cases (Fig. 1, Table 2). The tentorial notch was classified as typical in 6 patients and narrow in 2 (patients 6 and 9).

Four patients underwent central motor conduction studies with transcranial magnetic stimulation, which revealed alterations in corticospinal tract (CST) conduction contralateral to the lesion in 3 of them (patients 4, 9, and 11). In patient 12, the intraoperative study revealed transient, complete loss of motor evoked potentials (MEP) contralateral to the lesion in the first intervention, and a sudden, persistent loss of MEP in the left CST during the second surgical procedure (see Video in the Supplementary material).

Decompressive surgery was performed in 58.33% of patients; patient 12 underwent 2 surgeries, one following a supratentorial and the other an infratentorial approach. Follow-up time varied greatly, ranging from 7 days to one year (mean, 157 days). Motor function improved with respect to baseline in 7 patients. Regarding functional outcomes, 41.66% of patients scored 0-2 on the mRS. Surgery was contraindicated in 2 cases due to severe comorbidities (patients 6 and 7), and 4 patients died due to progression of the underlying disease or related complications (patients 1, 3, 4, and 5).

Discussion

Kernohan-Woltman notch phenomenon: an exceptional neurological picture?

Although it is difficult to establish the exact frequency of KWNP in clinical practice, the most recent literature reviews (which mainly include case reports) suggest that this is an exceptionally rare phenomenon.[4,5] However, in the light of the case series presented here, we believe that the incidence of KWNP may be underestimated. The number of original cases presented here is considerably higher than in previous studies, which underscores the need not only to raise awareness of this phenomenon among clinicians but also to perform detailed neurological examinations; this was already suggested nearly a century ago by the Belgian neurosurgeon Léon Ectors, a pioneer in the study of the association between KWNP and extra-axial expansive processes located in the greater wing of the sphenoid bone.[10]

Compared to historical series, where IH was mainly described in patients with intracranial neoplasia,[2,3] our series shows that this phenomenon most frequently develops rapidly, in the context of head trauma or intracranial haemorrhage (Table 1). It is therefore unsurprising that, in these patients, motor impairment (which is frequently bilateral) is accompanied by alterations in the level of consciousness and pupillary dysfunction; this stands in contrast with patients developing isolated IH secondary to a slower-growing expansive process.

Pathophysiological mechanisms of KWNP

A systematic review of historical series proposed 3 main pathophysiological mechanisms for IH[2] (Fig. 2): *1)* absence of CST decussation,[11] *2)* compression of the contralateral cerebral peduncle against the tentorial notch (ie, KWNP),[3,12,13] and *3)* diaschisis or dysfunction of the contralateral CST secondary to commissural fibre dysfunction.[14,15] Today, a wide range of tools (mainly MRI tractography and MEP studies) are available for differential diagnosis between the first 2 hypotheses, whereas the third possibility is difficult to confirm or rule out in clinical practice, although some authors continue to support it.[16,17]

Based on the imaging and neurophysiological study results from our series, we may conclude that all cases of IH were due to KWNP (Tables 1 and 2). In most cases, imaging studies revealed compression of the cerebral peduncle contralateral to the expansive process causing the symptoms, which in some cases was associated with an underlying structural lesion at that anatomical location (Table 2, Fig. 1, Supplementary material). It should be noted that the main innovation of the famous study published by Kernohan and Woltman[3] in 1929 was to demonstrate, in a series of cadavers, the presence of a notch, groove, or elastic deformation in the contralateral cerebral peduncle caused by compression against the tentorial edge.

Diagnosis of KWNP: characterisation of the peduncular lesion with MRI

In addition to the peduncular deformation, Kernohan and Woltman[3] identified a mesencephalic lesion underneath some of these grooves. From a microscopic viewpoint, the lesion was defined by myelin destruction and corticospinal fibre degeneration, of variable severity in both cases, and occasionally accompanied by focal haemorrhage.[3] This lesion, originally described by Groeneveld and Schaltenbrand[12] in 1927 and first demonstrated in MRI studies in 1990,[18] seems to represent the pathological substrate for the signal alterations detected with MRI in our series (Table 2, Fig. 1, Supplementary material). These peduncular lesions are frequently identified on MRI as an area of increased signal intensity at the ventrolateral peduncular edge on T2-weighted and FLAIR sequences, but are more difficult to detect with CT and on T1-weighted sequences due to their low density and signal intensity, respectively (Table 2, Fig. 1).[4,5,18,19] They are usually round or oval in axial slices, and may appear triangular in coronal slices.[4,5,18,19] We should point out that the most sensitive sequences are diffusion-weighted and diffusion tensor sequences, which can even identify lesions that are not visible on conventional or structural MRI sequences.[20–22]

Although the development of these peduncular lesions has historically been attributed to a purely compressive mechanism, Kernohan and Woltman[3] were unable to rule out the role of underlying ischaemic mechanisms. In fact, a recent study provided pathological evidence of the role of ischaemic events secondary to compression and/or distortion of perforating arteries originating from the posterior cerebral artery and/or the superior cerebellar artery; this may contribute to the polymorphism of peduncular lesions and to the variability in their topographical distribution and extension.[23,24] Furthermore, the presence of oedema or focal ischaemia may explain the observation of marked alterations in diffusion-weighted and diffusion tensor sequences, without this necessarily implying poor long-term motor prognosis, as prognosis ultimately depends on the severity of the structural lesion to CST axons.[21]

As an exception to the traditional pathophysiological model of the development of KWNP, 2 patients in our series who presented post-traumatic diffuse cerebral oedema without midline shift but who did display perimesencephalic cistern obliteration later developed peduncular lesions (patients 8 and 9, Tables 1 and 2).

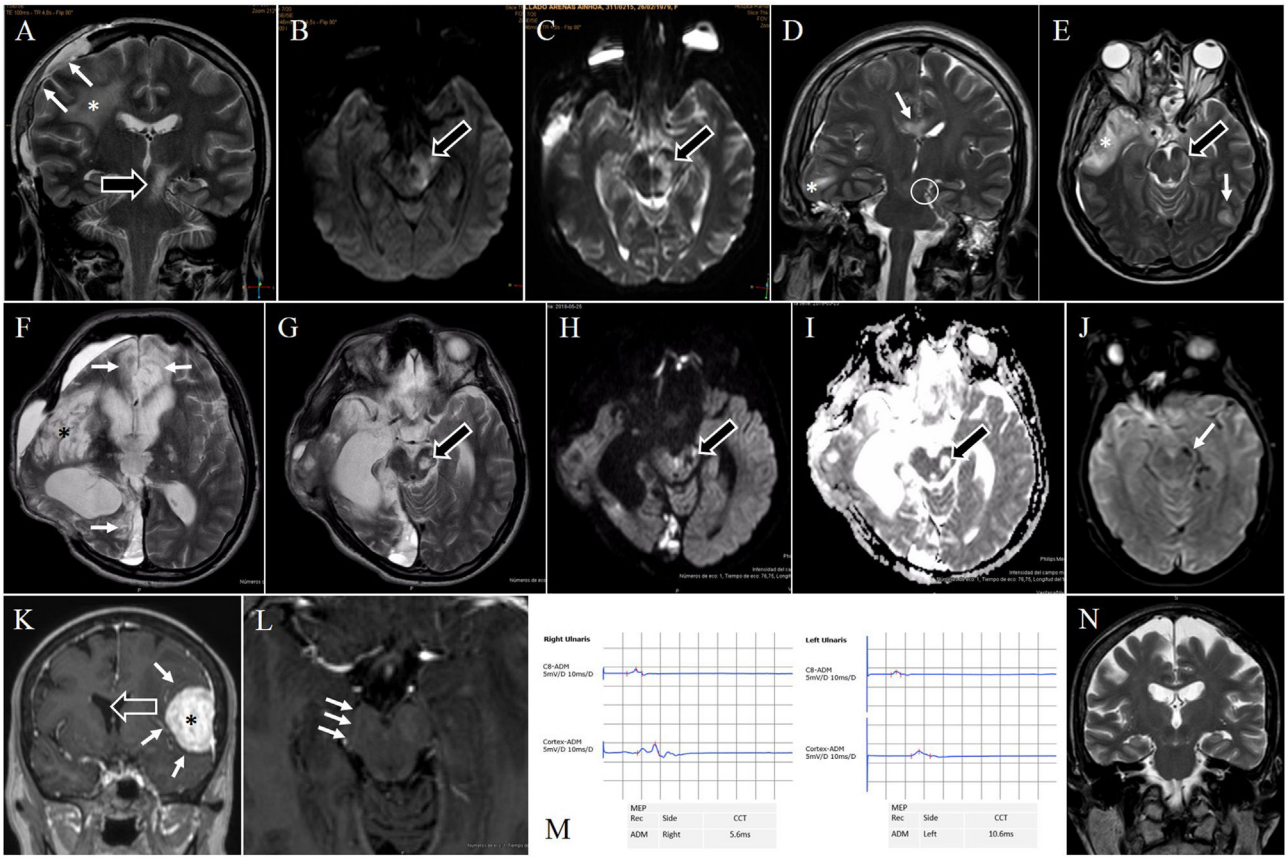

Figure 1 Selection of the most relevant findings from diagnostic studies in our series. **(A-C) Patient 1.** Brain MRI scan performed after right frontotemporoparietal craniectomy and drainage of an abscess in the right frontal lobe. A) T2-weighted sequence (coronal view) revealing residual oedema in the right frontal brain parenchyma (asterisk), with mild brain herniation through the craniectomy defect (white arrows), as well as a hyperintense lesion in the left cerebral peduncle (black arrow), located at the level of the tentorial notch and extending along the longitudinal axis. B) Diffusion-weighted sequence revealing signal hyperintensity involving the left midbrain nearly completely (arrow), with no evidence of diffusion restriction on the ADC map (C; arrow). **(D-E) Patient 2.** Postsurgical MRI scan, T2-weighted sequences (D: coronal view; E: axial view). Signal hyperintensity in the right temporal lobe, associated with contusion (asterisks in D and E). Residual tentorial notch in the left cerebral peduncle (white circle in D) associated with a hyperintense lesion at the ventrolateral edge of the peduncle (arrow in E). The MRI scan also revealed other hyperintense lesions involving the axons of the left posterior temporal corticosubcortical region and the corpus callosum (white arrows in D and E). **F-I) Patient 3.** Postsurgical MRI scan. F) T2-weighted sequence (axial view) at the level of the interventricular foramina, showing morphological alterations following decompressive craniectomy, with brain herniation through the bone defect and ventricular dilation associated with communicating hydrocephalus. The image also reveals signs of chronic ischaemia in the territories of both anterior cerebral arteries and the right posterior cerebral artery (white arrows in F), as well as malacia following the resolution of contusion foci in the right temporal lobe and insula (asterisk in F). G) T2-weighted sequence (axial view) at the level of the midbrain revealing a lesion in the central region of the left cerebral peduncle, with identical signal to that of cerebrospinal fluid on T2- and diffusion-weighted sequences and on ADC maps (black arrows in G, H, and I, respectively). **(J) Patient 8.** Magnetic susceptibility sequence showing haemosiderin deposition at the level of the lesion in the left cerebral peduncle (white arrow). **(K-N) Patient 11.** Preoperative MRI. A T1-weighted sequence following paramagnetic contrast administration (K: coronal view; L: axial view) showed an extra-axial expansive process in the greater wing of the left sphenoid bone (asterisk in K) associated with peripheral vasogenic oedema (white arrows in K), resulting in a mass effect with midline shift to the right (transparent arrow in K), causing deformation with flattening of the right cerebral peduncle secondary to compression against the tentorial notch (white arrows in L). A motor evoked potential study (M) revealed slower central conduction time and decreased amplitude in the right corticospinal tract (transcranial magnetic stimulation of the right motor cortex; recording in the left abductor minimi digiti). N) Follow-up MRI scan (coronal T2-weighted sequence) performed after surgical resection of meningioma, showing disappearance of the mass effect, with brain structures returning to the normal anatomical position, and no signs of structural lesions at the level of the right peduncle.

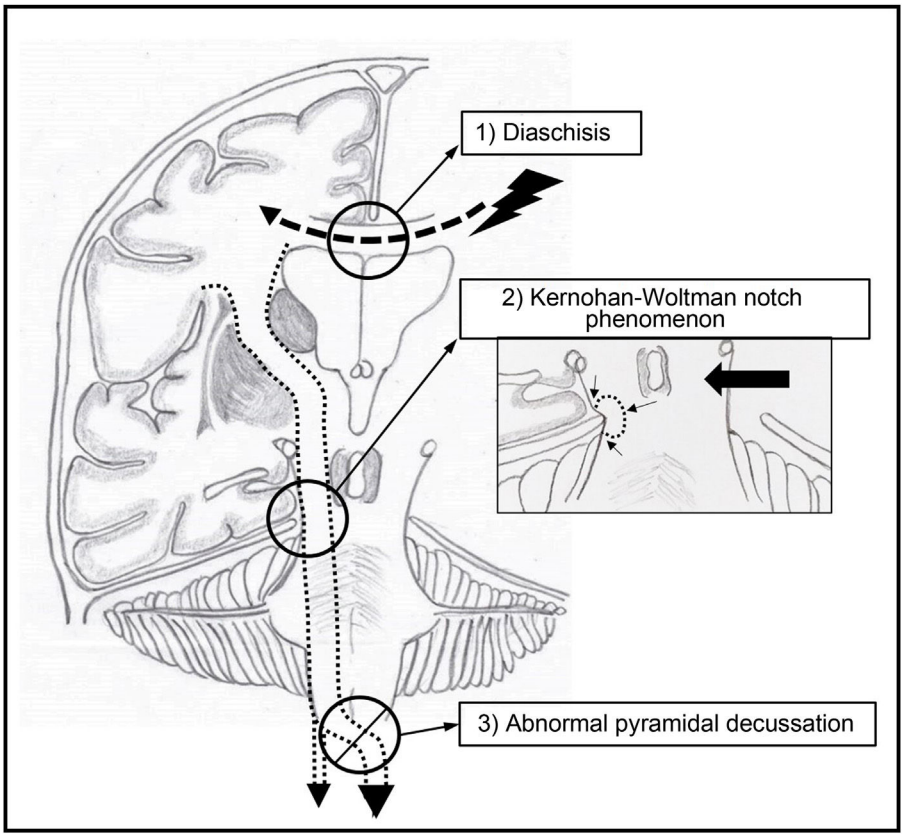

Figure 2 The main pathophysiological hypotheses for the development of ipsilateral hemiparesis.[2] Schematic representation of a coronal section of the brain: the dotted line represents the projection of the right corticospinal tract, with decussation at the level of the junction between the medulla oblongata and the spinal cord (the large arrowhead indicates the crossed pyramidal tract whereas the small arrowhead indicates the direct pyramidal tract). *1)* Theory of brain dysfunction caused by a remote brain lesion, proposed by the Mauritian physiologist and neurologist Charles-Édouard Brown-Séquard[14] (1817-1894), which served as the basis for the concept of diaschisis proposed by Constantin von Monakow (1853-1930). According to this concept, in the context of ipsilateral hemiparesis, a brain lesion affecting the primary motor area of the dominant hemisphere (black lightning symbol) may cause contralateral motor dysfunction secondary to impaired communication through the commissural fibres of the corpus callosum (black dashed arrow). *2)* Kernohan-Woltman notch phenomenon.[3] Brainstem displacement (solid black arrow) resulting in a groove in the cerebral peduncle caused by compression against the tentorial notch; it may be associated with a structural lesion to the corticospinal tract (dotted line and black arrows). *3)* Theory of the lack of decussation of corticospinal tract fibres,[11] demonstrated with the anatomoclinical method proposed by Albert Pitres (1848-1928) and Jean-Martin Charcot (1825-1893).

In similar cases, it has been suggested that the lesion may be explained by a dynamic pathophysiological mechanism consisting of rapid lateral displacement and compression of the peduncle against the tentorial edge.[2,25,26] We should also mention patient 12 from our series (Tables 1 and 2), who presented complete loss of MEP in the contralateral CTS during surgery for left petroclival meningioma; this was probably a iatrogenic complication of surgery, which translated clinically into postsurgical hemiplegia with rapid functional improvement in the immediate postoperative period (Supplementary material). This observation further supports the pathogenic role of dynamic factors in the development of peduncular compression,[27] and also points to the involvement of space-occupying lesions at the level of the tentorial notch[28] (in our patient, the tumour that motivated the intervention). We should be mindful that a narrow tentorial notch has traditionally been considered a predisposing factor for KWNP.[10,29] In our series, most patients in whom the tentorial notch was measured presented typical dimensions according to the classification of Adler and Milhorat[8] (Table 2). Although this classification constitutes the most detailed systematic description of this anatomical structure as compared to previous studies,[30–32] our data should be interpreted with caution due to the methodological particularities of the reference study[8] and the lack of similar studies in our setting.

Prognosis of ipsilateral hemiparesis secondary to Kernohan-Woltman notch phenomenon

Regarding the prognosis of motor function following KWNP, our series showed the reversible nature of the deficit in cases exclusively presenting an elastic deformation of the cerebral peduncle (patients 11 and 12). In patient 4, in contrast, deficits persisted in the immediate postoperative period; long-term follow-up data on motor function is not available. Motor function recovery was variable in patients presenting structural lesions involving the cerebral peduncle (Table 1). Several studies have shown the important role of cytotoxic oedema in the initial stages of peduncular lesions (both from a clinical and a radiological viewpoint), whereas the degree and severity of CST fibre involvement are determining factors in the irreversibility of IH and in functional prognosis.[21,22] To confirm or rule out this hypothesis, serial MRI studies including diffusion-weighted and diffusion tensor sequences should be

performed to establish a correlation between signs of a structural lesion to the cerebral peduncles and long-term clinical progression of motor deficits. The poor prognosis observed in our series (defined as high mRS scores) was influenced by the development of ischaemic lesions secondary to brain herniation (patient 3) or diffuse axonal lesions (patients 8 and 9); surgery was ruled out in 2 patients due to severe comorbidities (patients 6 and 7).

Conclusions

After thorough analysis of the clinical data, pathophysiological mechanisms, and neuroradiological and neurophysiological study results from a series of 12 patients with diagnosis of IH secondary to KWNP, we drew the following conclusions:

1. Compared to previously reported series, our series presents a higher frequency of KWNP secondary to head trauma and a lower frequency of KWNP secondary to tumours.
2. KWNP is frequently caused by compression (or contusion) of the cerebral peduncle against the tentorial notch, which may cause a structural lesion to the CST at this level.
3. Presence of a narrow tentorial notch and/or a pathological entity involving the area of this anatomical structure may predispose to KWNP.
4. MRI is the imaging technique of choice to confirm KWNP, particularly with diffusion-weighted and diffusion tensor sequences. MEP studies may help to support diagnosis of KWNP and rule out other mechanisms of IH.
5. The motor prognosis of patients with KWNP depends on the severity of CST axonal involvement. Larger studies with serial MRI scans and longer follow-up periods are needed to understand the nature, severity, and progression of peduncular lesions.

Acknowledgements

The authors wish to thank the library staff at Hospital Ramón y Cajal for their help in obtaining numerous documents used in this article.

Appendix A. Supplementary data

Supplementary data associated with this article can be found, in the online version, at http://dx.doi.org/10.1016/j.nrleng.2022.09.010.

References

1. Collier J. The false localising signs of intracranial tumour. Brain. 1904;27:490—508.
2. Carrasco-Moro R, Castro-Dufourny I, Martínez-San Millán JS, Cabañes-Martínez L, Pascual JM. Ipsilateral hemiparesis: the forgotten history of this paradoxical neurological sign. Neurosurgical Focus. 2019;47:E7, http://dx.doi.org/10.3171/2019.6.FOCUS19337.
3. Kernohan JW, Woltman HW. Incisura of the crus due to contralateral brain tumor. Arch Neurol Psychiatr. 1929;21:274—87.
4. Zhang CH, DeSouza RM, Kho JSB, Vundavalli S, Critchley G. Kernohan Woltman notch phenomenon: a review article. Br J Neurosurg. 2017;31:157—66, http://dx.doi.org/10.1080/02688697.2016.1211250.
5. Beucler N, Cungi PJ, Baucher G, Coze S, Dagain A, Roche PH. The Kernohan-Woltman Notch phenomenon: a systematic review of clinical and radiologic presentation, surgical management, and functional prognosis. J Korean Neurosurg Soc. 2022, http://dx.doi.org/10.3340/jkns.2022.0002.
6. Teasdale G, Maas A, Lecky F, Manley G, Stocchetti N, Murray G. The Glasgow Coma Scale at 40 years: standing the test of time. Lancet Neurol. 2014;13:844—54, http://dx.doi.org/10.1016/S1474-4422(14)70120-6.
7. Dyck PJ, Boes CJ, Mulder D, Millikan C, Windebank AJ, Dyck PJB, et al. History of standard scoring, notation, and summation of neuromuscular signs. A current survey and recommendation. J Peripher Nerv Sys. 2005;10:158—73, http://dx.doi.org/10.1111/j.1085-9489.2005.0010206.x.
8. Adler DE, Milhorat TH. The tentorial notch: anatomical variation, morphometric analysis, and classification in 100 human autopsy cases. J Neurosurg. 2002;96:1103—12, http://dx.doi.org/10.3171/jns.2002.96.6.1103.
9. Broderick JP, Adeoye O, Elm J. Evolution of the modified Rankin Scale and its use in future stroke trials. Stroke. 2017;48:2007—12, http://dx.doi.org/10.1161/STROKEAHA.117.017866.
10. Ectors L. Les méningiomes de la troisiéme frontale. Paris: Masson; 1945.
11. Charcot JM, Pitres A. Des observations contradictoires. In: Charcot JM, Pitres A, editors. Les centres moteurs corticaux chez l'homme. Paris: Rueff et Cie. Éditeurs; 1895. p. 183—91.
12. Groeneveld A, Schaltenbrand G. Ein Fall von Duraendotheliom über der Grosshirnhemisphäre mit einer bemerkenswerten komplikation: Läsion des gekreuzten Pes pedunculi durch Druck auf den Rand des Tentoriums. Dtsch Z Nervenheilkd. 1927;117:32—50.
13. Dammers R, Volovici V, Kompanje EJ. The history of the Kernohan Notch revisited. Neurosurgery. 2016;78:581—4, http://dx.doi.org/10.1227/NEU.0000000000001097.
14. Brown-Séquard CE. Recherches sur la physiologie et la pathologie de la protuberance annulaire. Journale de la Physiologie de l'Homme et des Animaux. 1858;1:523—39.
15. von Monakow C. Shock und diaschisis. In: von Monakow C, editor. Gehirnpathologie. Vienna: Alfred Hölder; 1905. p. 236—48.
16. Derakhshan I. The Kernohan—Woltman phenomenon and laterality of motor control: Fresh analysis of data in the article ''Incisura of the crus due to contralateral brain tumor''. J Neurol Sci. 2009;287:296, http://dx.doi.org/10.1016/j.jns.2009.07.015.
17. Derakhshan I. Transcranial motor evoked potential recording in a case of Kernohan's Notch syndrome: case report. Neurosurgery. 2005;56:E1166, http://dx.doi.org/10.1227/01.NEU.0000155092.23615.E3.
18. Cohen AR, Wilson J. Magnetic resonance imaging of Kernohan's notch. Neurosurgery. 1990;27:205—7, http://dx.doi.org/10.1097/00006123-199008000-00005.
19. Carrasco R, Pascual JM, Navas M, Martínez-Flórez P, Manzanares-Soler R, Sola RG. Kernohan-Woltman notch phenomenon caused by an acute subdural hematoma. J Clin Neurosci. 2009;16:1628—31, http://dx.doi.org/10.1016/j.jocn.2009.02.015.
20. Uesugi S, Suehiro E, Nakayama H, Suzuki M. Diffusion-weighted magnetic resonance imaging in a case of Kernohan's notch phenomenon. Acta Neurochir. 2010;152:1809—10, http://dx.doi.org/10.1007/s00701-010-0732-4.
21. Jang SG, Pyun SB. Diffusion tensor tractography in two cases of Kernohan-Woltman notch phenomenon. Ann Rehabil Med. 2013;37:879—85, http://dx.doi.org/10.5535/arm.2013.37.6.879.
22. Mansilla-Fernández B, Isla-Guerrero A, Giner J, Royo-Orejas A. Tractography in Kernohan's phenomenon: report of a case of acute subdural hematoma. Rev Neurol. 2015;60:286—7.

23. Hussain SI, Cordero-Tumangday C, Goldenberg FD, Wollman R, Frank JI, Rosengart AJ. Brain ischemia in acute herniation syndrome. J Clin Neurol Sci. 2008;268:190—2, http://dx.doi.org/10.1016/j.jns.2007.11.008.
24. Leever J. Unilateral cerebral herniation resulting in combined contralateral superior cerebellar artery territory infarction and mesencephalic injury: two cases of a severe unrecognized variant of Kernohan notch phenomenon? Radiol Cas Rep. 2020;15:250—3, http://dx.doi.org/10.1016/j.radcr.2019.12.004.
25. Eesa M, Bell K. Kernohan-Woltman notch phenomenon. J Trauma. 2010;69:1634, http://dx.doi.org/10.1097/TA.0b013e31818b2590.
26. Chang GY. Contusional Kernohan notch phenomenon. Neurol Clin Pract. 2016;6:553—4, http://dx.doi.org/10.1212/CPJ.0000000000000299.
27. Dyck P. Peduncular hemiplegia following removal of large cerebellopontine angle tumors: discussion of a mechanism of brainstem injury. Bull Los Angeles Neurol Soc. 1977;42:8—15.
28. Kahanov L, Hadelsberg UP, Kaye A, Spektor S, Valero F, Cohen J, et al. False lateralizing sign in skull base tumor a case series of five patients. Interdiscipl Neurosurg. 2021;26:101340, http://dx.doi.org/10.1016/j.inat.2021.101340.
29. Jones KM, Seeger JF, Yoshino MT. Ipsilateral motor deficit resulting from a subdural hematoma and a Kernohan's notch. AJNR. 1991;12:1238—9.
30. Sunderland S. The tentorial notch and complications produced by herniations of the brain through that aperture. Br J Surg. 1958;45:422—38, http://dx.doi.org/10.1002/bjs.18004519306.
31. Corsellis JA. Individual variation in the size of the tentorial opening. J Neurol Neurosurg Psychiatry. 1958;21:279—83, http://dx.doi.org/10.1136/jnnp.21.4.279.
32. Ono M, Ono M, Rothon AL, Barry M. Microsurgical anatomy of the region of the tentorial incisura. J Neurosurg. 1984;60:365—99, http://dx.doi.org/10.3171/jns.1984.60.2.0365.